Alignment tolerances for plane wave to single-mode fiber coupling and their mitigation by use of pigtailed collimators

Oswald Wallner, Peter J. Winzer, Walter R. Leeb

Institut für Nachrichtentechnik und Hochfrequenztechnik,

Technische Universität Wien, Gusshausstrasse 25/389,

A-1040 Vienna, Austria

oswald.wallner@ieee.org

We discuss the efficiency with which coherent plane waves can be coupled to single-mode fibers in the presence of deterministic or stochastic misalignments of the fiber relative to the lens' focal point. We point out how the alignment demands can be relaxed by means of GRIN-lens fiber-pigtailed collimators.

OCIS codes: 060.2430,120.1680,120.4820

1 Introduction

Efficient coupling of coherent plane waves to single-mode fibers is required for a growing number of optical instruments, e.g. for free-space optical communication systems. Any de-

viation from the optimum coupling geometry, e.g. fiber misalignment concerning lateral or axial positioning, or any fiber tilt, may reduce considerably the power coupled into the fiber. This subject has been extensively studied for the coupling of coherent Gaussian beams[1–5] as well as of incoherent radiation.[6–10] For the case of coherent plane wave coupling[11,12] the important interplay between angular and lateral misalignment does not seem to have been sufficiently studied.

In this paper we thus investigate the influence of deterministic and stochastic misalignment on coherent plane wave to single-mode fiber coupling. Section **2** is devoted to conventional coupling by means of a bulk lens system. We define a design parameter χ which, when optimized, leads to the well-known maximum coupling efficiency $\eta_0 = 81\%$. For three types of misalignment – lateral and axial misplacement, as well as fiber tilt – we perform both a deterministic and a stochastic analysis for individual and combined degradations, and find the corresponding coupling efficiencies. In Sec. **3**, we calculate the potential relaxation on alignment tolerances by adding a fiber-pigtailed collimator lens. With the design parameter χ optimized, the lateral alignment requirements are relaxed at the expense of a more accurate angular positioning as well as of a larger focal length of the primary (bulk) coupling lens.

2 Conventional coupling

We model conventional coupling as shown in Fig.1. A freely propagating wave is focussed by a thin, diffraction limited lens of focal length f and clear aperture radius a located in the aperture plane $\mathcal{A}$ at $z = 0$. The bare fiber end is placed close to the focal plane, i.e. at a distance $z = f + \triangle z$ in the coupling plane $\mathcal{B}$. In the aperture plane we describe

the complex incident field by $E_{\mathcal{A}}(x,y)$, in the coupling plane we denote its corresponding complex conjugate $E^*_{\mathcal{B}}(x,y)$. If the fundamental mode of the single-mode fiber is described by $F_{\mathcal{B}}(x,y)$, the power coupled into the fiber, P_f, is determined by the squared modulus of the overlap integral of $E^*_{\mathcal{B}}(x,y)\cdot F_{\mathcal{B}}(x,y)$ in the coupling plane $\mathcal{B}$.

The coupling efficiency η is defined[1] as the ratio of P_f to the power available in the aperture plane, $P_{av} = \iint_{\mathcal{A}} |E_{\mathcal{A}}(x,y)|^2\, dxdy$. Generally, η can be evaluated in any plane between $\mathcal{A}$ and $\mathcal{B}$, with the optical fields properly transformed. In the present case it is convenient to perform the overlap integral in the aperture plane, which leads to

$$\eta = \frac{\left|\iint_{\mathcal{A}} E^*_{\mathcal{A}}(x,y)\cdot F_{\mathcal{A}}(x,y)\, dxdy\right|^2}{\iint_{\mathcal{A}} |E_{\mathcal{A}}(x,y)|^2\, dxdy} \quad , \tag{1}$$

where $F_{\mathcal{A}}(x,y)$ is the fiber's eigenmode, backpropagated[13] to the aperture plane and normalized as $\iint_{\mathcal{A}} |F(x,y)|^2\, dxdy = 1$.

In practice, perfect alignment of the fiber relative to the lens will not be achieved, resulting in a modification of the backpropagated fiber mode $F_{\mathcal{A}}(x,y)$ and, consequently, in a reduced coupling efficiency $\eta < \eta_0$. We investigate the influence of the following three fundamental types of misalignment:

1. *Lateral offset*, $\triangle x$ and $\triangle y$, of the fiber axis from the lens' optical axis in the coupling plane. This results in a modification of the phase front curvature of the backpropagated fiber mode, leading to an additional factor of $\exp\left[2\pi\left(x\cdot\triangle x/(\lambda f) + y\cdot\triangle y/(\lambda f)\right)\right]$ in the expression for $F_{\mathcal{A}}$.

2. *Fiber tilt* by angles $\triangle\varphi_x$ and $\triangle\varphi_y$ in the xz-plane and the yz-plane, respectively. In the aperture plane $\mathcal{A}$ this results in a lateral shift of the backpropagated mode $F_{\mathcal{A}}$ by $\triangle\varphi_x f$ and $\triangle\varphi_y f$.

3. *Defocus* $\triangle z$ of the fiber-lens system. A small defocus ($\triangle z \ll f$) causes an additional phase front curvature of $F_{\mathcal{A}}$, described by a factor $\exp\left[-j\pi\triangle z/(\lambda f^2)\right]$.

In most practical cases the coupling plane $\mathcal{B}$ lies in the Fresnel region of the lens,[14] and fields of non-negligible intensity extend only to lateral dimensions small compared to the distance between $\mathcal{A}$ and $\mathcal{B}$. If we further approximate the fiber's eigenmode by a Gaussian field distribution[15] with modefield radius $w_{\mathcal{B}}$ ($1/e^2$ intensity), the backpropagated fiber mode is easily found to be

$$F_{\mathcal{A}}(x,y) = \sqrt{\frac{2}{\pi w_{\mathcal{A}}^2}} \cdot \exp\left[-\left(\frac{1}{w_{\mathcal{A}}^2} - j\frac{\pi\triangle z}{\lambda f^2}\right)\left((x-\triangle\varphi_x f)^2 + (y-\triangle\varphi_y f)^2\right)\right] \times \exp\left[j2\pi\left(\frac{\triangle x}{\lambda f}(x-\triangle\varphi_x f) + \frac{\triangle y}{\lambda f}(y-\triangle\varphi_y f)\right)\right] \quad , \quad (2)$$

where λ is the wavelength and $w_{\mathcal{A}}$ is the modefield radius of the backpropagated fiber mode, given by $w_{\mathcal{A}} = \lambda f/(\pi w_{\mathcal{B}})$.

A Deterministic case

For a plane input field $E_{\mathcal{A}}$, resulting in an Airy-distribution in the coupling plane $\mathcal{B}$, inserting (2) in (1) yields

$$\eta = \left|\frac{\sqrt{2}}{\pi\chi}\iint\limits_{\mu^2+\nu^2\le\chi^2} \exp\left[-\left(1-j\frac{\triangle z'}{\chi}\right)\left((\mu-\chi\triangle\varphi'_x)^2 + (\nu-\chi\triangle\varphi'_y)^2\right)\right] \times \exp\left[j2\left(\triangle x'\mu + \triangle y'\nu\right)\right] d\mu d\nu\right|^2 \quad , \quad (3)$$

where the offsets are normalized as given in Table 1. In Eq. 3 the design parameter $\chi = a/w_{\mathcal{A}}$ was introduced as the ratio of the aperture radius to the radius of the backpropagated fiber mode.

Optimum coupling can be achieved if the fiber end face is located in the focal plane ($\triangle z = 0$) with zero lateral misalignment ($\triangle x = \triangle y = 0$) and no fiber tilt ($\triangle\varphi_x = \triangle\varphi_y = 0$). In this case, Eq. 3 yields

$$\eta = \frac{2}{\chi^2}\left(1 - e^{-\chi^2}\right)^2 \quad . \tag{4}$$

The function $\eta(\chi)$ exhibits a rather broad maximum, where an optimum coupling efficiency[12] of $\eta_0 = 81\%$ is obtained for a design parameter of $\chi_0 = 1.121$.

A numerical evaluation of Eq. 3 for individual misalignments is given in Fig. 2. Figure 2(a) and (b) show the dependence of the coupling efficiency on lateral misalignment $\triangle x'$ and tilt $\triangle\varphi'_x$, respectively, for optimized design parameter $\chi = \chi_0$ and for the case $\chi = 0.7\chi_0$. The following key results can be read from these figures:

a) Accurate lateral positioning is particularly critical for efficient coupling, as already a lateral offset $\triangle x$ equal to one mode field radius reduces the efficiency to approximately one third of the theoretically maximum value. (One should have in mind that for a standard single-mode fiber the mode field radius is approximately $5\mu m$.)

b) Even a fiber tilt as large as half the inverse F-number, a/f, reduces the efficiency only by about a quarter of the maximum value. (A typical value for a/f might be 0.2, corresponding to an angle of 11.5°.)

c) A sub-optimum design parameter ($\chi < \chi_0$) leads to improved coupling efficiency if the misalignment parameter is relatively large. The reason is that a smaller design parameter yields an increased spot size $w_{\mathcal{A}}$ of the backpropagated fiber mode, which obviously relaxes the tolerances.

The demands on accurate axial positioning, not shown here, are less severe; even a normalized defocus of three reduces the coupling efficiency only to about half of the maximum value.

In an actual setup, lateral offset and fiber tilt will occur simultaneously. Figure 3 shows contour lines of constant coupling efficiency as a function of both these parameters. The two sets of lines correspond to the design parameters $\chi = \chi_0$ and $\chi = 0.7\chi_0$. If a certain value of η ($< \eta_0$) is required, the lateral alignment tolerance can be relaxed at the expense of tilt tolerance, as expected. With the help of Figs. 2 and 3, one may show that the combined effect of lateral and tilt misalignment on coupling efficiency can be approximated quite well by multiplying the normalized coupling efficiencies due to each individual misalignment, i.e. $\eta(\triangle x', \triangle\varphi'_x)/\eta_0 \approx \eta(\triangle x')/\eta_0 \cdot \eta(\triangle\varphi'_x)/\eta_0$, if the deviations $1 - \eta/\eta_0$ are much smaller than unity.

B Stochastic case

In many applications it will be more relevant to consider the values of the misalignment parameters to be of stochastic nature. Such a view is, e.g., adequate if the mutual alignment of lens and fiber end is subject to environmental disturbances, or in case that the alignment is aided by control loops exhibiting non-negligible noise. The coupling efficiency $\boldsymbol{\eta}$ will then be a random variable. (Bold print indicates random quantities throughout this work.)

We assume that the normalized lateral offsets ($\boldsymbol{\Delta x}'$, $\boldsymbol{\Delta y}'$) and the normalized tilts ($\boldsymbol{\Delta\varphi}'_x$, $\boldsymbol{\Delta\varphi}'_y$) are zero-mean Gaussian random variables. Because of the less critical dependence of the coupling efficiency on the (normalized) defocus $\triangle z'$, we assume it to be of deterministic nature. If we suppose the random variables describing the individual misalignments to be

statistically independent, the mean coupling efficiency is given by (see Appendix A)

$$\begin{aligned}\langle\boldsymbol{\eta}\rangle = \frac{2}{(\pi\chi)^2}\cdot\iint_{\mathcal{Q}}\iint_{\tilde{\mathcal{Q}}}\exp\left[-\left(\mu^2+\nu^2+\tilde{\mu}^2+\tilde{\nu}^2\right)+j\frac{\triangle z'}{\chi}\left(\mu^2+\nu^2-\tilde{\mu}^2-\tilde{\nu}^2\right)\right]\\ \times\exp\left[2\chi^2\left(\mu+\tilde{\mu}-j\frac{\triangle z'}{\chi}(\mu-\tilde{\mu})\right)^2\sigma^2_{\triangle\varphi'_x}\Big/\left(1+4\chi^2\sigma^2_{\triangle\varphi'_x}\right)\right]\Big/\sqrt{1+4\chi^2\sigma^2_{\triangle\varphi'_x}}\\ \times\exp\left[2\chi^2\left(\nu+\tilde{\nu}-j\frac{\triangle z'}{\chi}(\nu-\tilde{\nu})\right)^2\sigma^2_{\triangle\varphi'_y}\Big/\left(1+4\chi^2\sigma^2_{\triangle\varphi'_y}\right)\right]\Big/\sqrt{1+4\chi^2\sigma^2_{\triangle\varphi'_y}}\\ \times\exp\left[-2\left(\mu-\tilde{\mu}\right)\sigma^2_{\triangle x'}-2\left(\nu-\tilde{\nu}\right)\sigma^2_{\triangle y'}\right]d\mu\,d\nu\,d\tilde{\mu}\,d\tilde{\nu}\quad,\quad(5)\end{aligned}$$

where the symbols $\mathcal{Q}$ and $\tilde{\mathcal{Q}}$ denote circular areas of integration, namely $\mathcal{Q}=\mu^2+\nu^2\le\chi^2$ and $\tilde{\mathcal{Q}}=\tilde{\mu}^2+\tilde{\nu}^2\le\chi^2$.

Figures 4(a) and (b) present the normalized mean coupling efficiency $\langle\boldsymbol{\eta}\rangle/\eta_0$ as a function of the standard deviations $\sigma_{\triangle x'}$ and $\sigma_{\triangle\varphi'_x}$ for $\chi=\chi_0$ and $\chi=0.7\chi_0$, both for focal coupling ($\triangle z=0$). One should compare these results with those presented in Figs. 2(a) and (b), covering the deterministic case. As expected, in both cases the coupling efficiency has identical values for zero misalignment. However, a non-optimized design parameter χ will now be of less benefit in case of large misalignment. Also, the mean value $\langle\boldsymbol{\eta}\rangle$ in the stochastic case is always larger than (or, at the worst, equal to) the deterministic value η for a standard deviation equal to the deterministic misalignment.

The simultaneous occurrence of lateral and tilt misalignment is covered by Fig. 5 and should be compared to its deterministic counterpart, Fig. 3.

3 Coupling with a fiber collimator

As indicated in Sec. **2**, the critical part of adjusting a standard fiber in practice is rather the lateral direction than the tilt. It would thus be desirable to reduce the tolerance requirements

concerning lateral adjustment at the expense of those for tilt. Figures 3 and 5 show that such a trade-off between lateral and tilt tolerance is indeed possible and requires an increase of the modefield radius in the coupling plane.

One method to increase the modefield radius is to attach a quarter-pitch GRIN lens[16] to the fiber end, which acts as a collimator. An incident beam with spot size $w_{\mathcal{C}}$ and plane wavefront (as may be produced by a conventional lens in its focal plane), is then transformed into a beam with a plane wavefront of spot size $w_{\mathcal{B}}$.

In the following, we describe the quantitative consequences of employing a fiber-pigtailed collimator instead of a bare fiber end (see Fig. 6). We denote the magnification factor, which increases the modefield radius, by $A = w_{\mathcal{C}}/w_{\mathcal{B}}$. Keeping in mind that the design parameter $\chi = (\pi a w_{\mathcal{C}})/(\lambda f_{\mathcal{C}})$ should be kept close to its optimum value $\chi_0 = 1.121$, an increase of the modefield radius by a factor A asks for increasing f by the same factor. This will result in a new focal length of $f_{\mathcal{C}} = A \cdot f$ if we suppose that the lens' size (radius a) has to stay unchanged. The new tolerances concerning lateral alignment, $\triangle x' = \triangle x/w_{\mathcal{C}}$ and $\triangle y' = \triangle y/w_{\mathcal{C}}$, are relaxed by the factor A, while those for the tilt, $\triangle \varphi'_x = \triangle \varphi_x/(a/f_{\mathcal{C}})$ and $\triangle \varphi'_y = \triangle \varphi_y/(a/f_{\mathcal{C}})$, are tightened by A. The tolerance concerning defocus, $\triangle z' = \triangle z \cdot a/(f_{\mathcal{C}} w_{\mathcal{C}})$, is relaxed by the square of the magnification factor.

Figure 7 illustrates the influence of a variation in the magnification factor A on misalignment tolerances. Lines of mean coupling efficiency $\langle \boldsymbol{\eta} \rangle = 0.75\eta_0$ are drawn as a function of the standard deviations $\sigma_{\triangle x}$ and $\sigma_{\triangle \varphi_x}$ of the normalized lateral misalignment and of normalized tilt. The defocus $\triangle z$ is assumed to be zero. One finds, e.g., that in case that a standard deviation of the lateral misalignment of less than $\sigma_{\triangle x} = w_{\mathcal{B}}$ cannot be guaranteed, a collimator with a magnification $A > 1.7$ is required to allow also for some tilt uncertainty.

To give a numerical example, we consider an optimized system ($\chi = \chi_0$) at a wavelength of $\lambda = 1.55\,\mu m$. The lens has a clear aperture radius $a = 1.25\,cm$ and a focal length $f = 11\,cm$, and the fiber's modefield radius is $w_{\mathcal{B}} = 5\,\mu m$. From Fig. 5 it follows that if a lateral misalignment standard deviation of half a modefield radius can be guaranteed, $\sigma_{\triangle x} = w_{\mathcal{B}}/2 = 2.25\,\mu m$, a tilt standard deviation of about $\sigma_{\triangle\varphi'_x} = 0.25$ (corresponding to $\sigma_{\triangle\varphi_x} = 1.6°$) is allowed to obtain a mean coupling efficiency of $\langle\boldsymbol{\eta}\rangle = 0.75\eta_0 = 61\%$. The tight tolerance concerning lateral positioning may be relaxed by, e.g., a factor of two to $\sigma_{\triangle x} = w_{\mathcal{B}} = 5\,\mu m$ by increasing the modefield radius by a factor $A = 3$, see Fig. 7. In this case a maximum tilt standard deviation of $\sigma_{\triangle\varphi'_x} = 0.13$, corresponding to $\sigma_{\triangle\varphi_x} = 0.9°$, is allowed for a minimum mean coupling efficiency of 61%. Note that the lens' focal length has to be increased by the same factor $A = 3$, i.e. to $f_{\mathcal{C}} = 33\,cm$.

One practical disadvantage of using a pigtailed collimator is the increase of the focal length, $f_{\mathcal{C}} = A \cdot f$, which is necessary for maximum coupling. The axial dimension ($\approx f_{\mathcal{C}}$) of the setup consisting of the (conventional) lens and of the GRIN-lensed fiber end might become unduly large, thus reducing the mechanical stability of the system and increasing alignment uncertainty. One could imagine a reduction of the system length by employing a defocused system, where the GRIN-lens is not placed into the focal plane ($z = f_{\mathcal{C}}$) but at a smaller distance. The curvature of the input field impinging on the GRIN-lens could be compensated by using a GRIN-lens with a correspondingly curved input face. However, our investigations along these lines[18] have shown that such an arrangement – although yielding optimum coupling for perfect alignment – would require a very high conformity of the wavefront curvature and the GRIN-lens curvature, which makes the defocused arrangement impractical with respect to lateral and angular misalignments.

4 Conclusions

We have discussed the effect of deterministic and stochastic fiber misalignment on the plane wave-to-single-mode fiber coupling efficiency. We have shown that a fiber-pigtailed collimator may relax the tolerance on lateral alignment at the expense of a smaller allowable fiber tilt. This will generally be advantageous in typical applications, however, it is accompanied by an increase in overall system length.

The authors are grateful to A. Kalmar for valuable discussions.

A Appendix: Calculation of mean coupling efficiency

The normalized lateral offsets ($\boldsymbol{\Delta x}'$, $\boldsymbol{\Delta y}'$) and the normalized tilts ($\boldsymbol{\Delta\varphi}'_x$, $\boldsymbol{\Delta\varphi}'_y$) are assumed to be zero-mean Gaussian random variables with standard deviations σ. For, e.g., the lateral offset in x-direction, $\boldsymbol{\Delta x}$, the probability density function is given by

$$p_{\boldsymbol{\Delta x}}(\triangle x) = \frac{1}{\sqrt{2\pi}\sigma_{\triangle x}} \exp\left[-\frac{1}{2}\left(\frac{\triangle x}{\sigma_{\triangle x}}\right)^2\right] \quad . \tag{6}$$

The mean coupling efficiency, $\langle\boldsymbol{\eta}\rangle$, is then defined by[17]

$$\langle\boldsymbol{\eta}\rangle = \iiiint \eta(\boldsymbol{\Delta x}, \boldsymbol{\Delta y}, \boldsymbol{\Delta\varphi}_x, \boldsymbol{\Delta\varphi}_y, \triangle z) \times p_{\boldsymbol{\Delta x},\boldsymbol{\Delta y},\boldsymbol{\Delta\varphi}_x,\boldsymbol{\Delta\varphi}_y}(\triangle x, \triangle y, \triangle\varphi_x, \triangle\varphi_y)\, d\triangle x\, d\triangle y\, d\triangle\varphi_x\, d\triangle\varphi_y \quad , \tag{7}$$

where p is the joint probability density function of all stochastically varying misalignment parameters. If we assume the random variables describing the individual misalignments to be statistically independent, the joint probability density function characterizing the combined statistics of the misalignments factorizes into the product of the individual probability density functions which each describe the statistics of a single imperfection, i.e.

$$p_{\boldsymbol{\Delta x},\boldsymbol{\Delta y},\boldsymbol{\Delta\varphi}_x,\boldsymbol{\Delta\varphi}_y}(\triangle x, \triangle y, \triangle\varphi_x, \triangle\varphi_y) = p_{\boldsymbol{\Delta x}}(\triangle x) \cdot p_{\boldsymbol{\Delta y}}(\triangle y) \cdot p_{\boldsymbol{\Delta\varphi}_x}(\triangle\varphi_x) \cdot p_{\boldsymbol{\Delta\varphi}_y}(\triangle\varphi_y) \tag{8}$$

In order to calculate $\langle\boldsymbol{\eta}\rangle$ we start with Eq. 3, assume stochastic misalignment parameters (except for the axial misplacement $\triangle z'$), and write

$$\langle\boldsymbol{\eta}\rangle = \left\langle \left| \frac{\sqrt{2}}{\pi\chi} \iint\limits_{\mu^2+\nu^2\le\chi^2} \exp\left[-\left(1 - j\frac{\triangle z'}{\chi}\right)\left((\mu - \chi\boldsymbol{\Delta\varphi}'_x)^2 + (\nu - \chi\boldsymbol{\Delta\varphi}'_y)^2\right)\right] \times \exp\left[j2\left(\boldsymbol{\Delta x}'\mu + \boldsymbol{\Delta y}'\nu\right)\right] d\mu d\nu \right|^2 \right\rangle \quad . \tag{9}$$

To make use of the linearity of the expectation operator $\langle\cdot\rangle$, we first write the squared modulus of Eq. 9 as a product of the form $|f(x)|^2 = f(x)f^*(x)$, and get, as a result of the statistical independence of the individual misalignment parameters,

$$\begin{aligned}\langle\boldsymbol{\eta}\rangle = \frac{2}{(\pi\chi)^2}\cdot\iint_{\mathcal{Q}}\iint_{\tilde{\mathcal{Q}}}\exp\left[-\left(\mu^2+\nu^2+\tilde{\mu}^2+\tilde{\nu}^2\right)+j\frac{\triangle z'}{\chi}\left(\mu^2+\nu^2-\tilde{\mu}^2-\tilde{\nu}^2\right)\right]\\ \times\left\langle\exp\left[-2\chi^2\left(\boldsymbol{\Delta\varphi}_x'^{\,2}-\left(\mu+\tilde{\mu}-j\frac{\triangle z'}{\chi}(\mu-\tilde{\mu})\right)\frac{1}{\chi}\boldsymbol{\Delta\varphi}_x'\right)\right]\right\rangle_{\boldsymbol{\Delta\varphi}_x'}\\ \times\left\langle\exp\left[-2\chi^2\left(\boldsymbol{\Delta\varphi}_y'^{\,2}-\left(\nu+\tilde{\nu}-j\frac{\triangle z'}{\chi}(\nu-\tilde{\nu})\right)\frac{1}{\chi}\boldsymbol{\Delta\varphi}_y'\right)\right]\right\rangle_{\boldsymbol{\Delta\varphi}_y'}\\ \times\left\langle\exp\left[j2\left(\mu-\tilde{\mu}\right)\boldsymbol{\Delta x}'\right]\right\rangle_{\boldsymbol{\Delta x}'}\cdot\left\langle\exp\left[j2\left(\nu-\tilde{\nu}\right)\boldsymbol{\Delta y}'\right]\right\rangle_{\boldsymbol{\Delta y}'}\,d\mu\,d\nu\,d\tilde{\mu}\,d\tilde{\nu}\quad.\end{aligned}\tag{10}$$

The symbols $\mathcal{Q}$ and $\tilde{\mathcal{Q}}$ denote circular areas of integration, namely $\mathcal{Q} = \mu^2+\nu^2 \le \chi^2$ and $\tilde{\mathcal{Q}} = \tilde{\mu}^2+\tilde{\nu}^2 \le \chi^2$, and $\langle\cdot\rangle_{\boldsymbol{\Delta x}'}$ means calculating the expected value with respect to the stochastic parameter $\boldsymbol{\Delta x}'$. The individual expected values can be easily calculated by using the relations

$$\left\langle\exp\left[-b(a\boldsymbol{x}+\boldsymbol{x}^2)\right]\right\rangle_{\boldsymbol{x}} = \exp\left[a^2b^2\sigma_x^2/(2+4b\sigma_x^2)\right]/\sqrt{1+2b\sigma_x^2}\tag{11}$$

$$\left\langle\exp\left[ja\boldsymbol{x}\right]\right\rangle_{\boldsymbol{x}} = \exp\left[-a^2\sigma_x^2/2\right]\quad,\tag{12}$$

yielding Eq. 5.

References

1. R.E. Wagner, W.J. Tomlinson, "Coupling efficiency of optics in single-mode fiber components," Appl. Opt. **21**, 2671–2688 (1982).

2. T. Takenaka et al., "Signal-to-noise ratio in optical heterodyne detection for Gaussian fields," Appl. Opt. **17**, 3466–3471 (1978)

3. K.A. Winick, P. Kumar, "Spatial Mode Matching Efficiencies for Heterodyned GaAlAs Semiconductor Lasers," Journal of Lightwave Technology **6**, 513–520 (1988)

4. K. Tanaka, N. Ohta, "Effects of tilt and offset of signal field on heterodyne efficiency," Appl. Opt. **26**, 627–632 (1987)

5. S. Yuan, N.A. Riza, "General formula for coupling-loss characterization of single-mode fiber collimators by use of gradient-index rod lenses," Appl. Opt. **38**, 3214–3222 (1999)

6. P.J. Winzer, W.R. Leeb, "Fiber coupling efficiency for random light and its applications to lidar," Opt. Lett. **23**, 986–988 (1998)

7. D.K. Jacob , "Heterodyne ladar system efficiency enhancement using single-mode optical fiber mixers," Optical Engineering **34**, 3122–3129 (1995)

8. R.G. Frehlich, M.J. Kavaya, "Coherent laser radar performance for general atmospheric refractive turbulence," Appl. Opt. **30**, 5325–5352 (1991)

9. J.Y. Wang, "Detection efficiency of coherent optical radar," Appl. Opt. **23**, 3421–3427 (1984)

10. G.D. Spiers, "The Effect Of Aberrations On The Performance Of A Coherent Doppler Lidar," 10th Biennial Coherent Laser Radar Technology and Applications Conference, Mt. Hood, Oregon, 1999

11. S.C. Cohen, "Heterodyne detection: phase front alignment, beam spot size, and detector uniformity," Appl. Opt. **14**, 1953–1959 (1975).

12. C. Ruilier, "A study of degraded light coupling into single-mode fibers," Proc. SPIE **3350**, 319–329 (1998)

13. A.E. Siegman, "The antenna properties of optical heterodyne receivers", Appl. Opt. **5**, 1588–1594 (1966)

14. K. Iizuka, *Engineering Optics* (Springer, Berlin, 1987)

15. J.A. Buck, *Fundamentals of Optical Fibers* (John Wiley & Sons, Inc., New York, 1995)

16. E.-G. Neumann, *Single-Mode Fibers* (Springer, Berlin, 1988)

17. A. Papoulis, *Probability, Random Variables, and Stochastic Processes* (McGraw-Hill, New York, 1991)

18. O. Wallner, *Kopplung ebener Wellen in Monomode-Glasfasern*, Diploma Thesis, Vienna Uni-

versity of Technology, 2000

Table 1. Normalized misalignment parameters.

	actual	normalized
lateral offset	$\triangle x$	$\triangle x' = \frac{\triangle x}{w_{\mathcal{B}}}$
	$\triangle y$	$\triangle y' = \frac{\triangle y}{w_{\mathcal{B}}}$
tilt	$\triangle \varphi_x$	$\triangle \varphi'_x = \frac{\triangle \varphi_x}{a/f}$
	$\triangle \varphi_y$	$\triangle \varphi'_y = \frac{\triangle \varphi_y}{a/f}$
defocus	$\triangle z$	$\triangle z' = \triangle z \frac{a}{f w_{\mathcal{B}}}$

Fig. 1. Coupling geometry. A thin lens of focal length f and clear aperture radius a focuses the incident field $E_{\mathcal{A}}(x, y)$ onto the bare end of a single-mode fiber, generating a field $E_{\mathcal{B}}(x, y)$ in the coupling plane $\mathcal{B}$ at $z = f + \triangle z$. The field resulting from backpropagating the fiber's fundamental mode $F_{\mathcal{B}}(x, y)$ (modefield radius $w_{\mathcal{B}}$) into the aperture plane $\mathcal{A}$ is designated $F_{\mathcal{A}}(x, y)$.

Fig. 2. Coupling efficiency η normalized to the maximum value $\eta_0 = 0.81$ for deterministic misalignment for optimal (χ_0) and sub-optimal ($\chi = 0.7\chi_0$) design parameter χ. (a) for normalized lateral misalignment $\triangle x' = \triangle x / w_{\mathcal{B}}$, (b) for normalized tilt $\triangle \varphi'_x = \triangle \varphi_x / (a/f)$.

Fig. 3. Contour lines of constant normalized coupling efficiency η/η_0 as a function of normalized lateral misalignment $\triangle x' = \triangle x / w_{\mathcal{B}}$ and normalized tilt $\triangle \varphi'_x = \triangle \varphi_x / (a/f)$ for deterministic parameters. Solid lines are for an optimum design parameter $\chi = \chi_0$, broken lines are for $\chi = 0.7\chi_0$.

Fig. 4. Mean coupling efficiency $\langle \boldsymbol{\eta} \rangle$ normalized to the maximum value $\eta_0 = 0.81$ for stochastic misalignment for optimal (χ_0, solid line) and sub-optimal ($\chi = 0.7\chi_0$, broken line) design parameter χ. (a) for normalized lateral misalignment $\boldsymbol{\Delta x'} = \boldsymbol{\Delta x}/w_{\mathcal{B}}$ with standard deviation $\sigma_{\triangle x'}$, (b) for normalized tilt $\boldsymbol{\Delta \varphi'}_x = \boldsymbol{\Delta \varphi}_x/(a/f)$ with standard deviation $\sigma_{\triangle \varphi'_x}$.

Fig. 5. Contour lines of constant normalized mean coupling efficiency $\langle \boldsymbol{\eta} \rangle / \eta_0$ as a function of normalized lateral misalignment $\boldsymbol{\Delta x'} = \boldsymbol{\Delta x}/w_{\mathcal{B}}$ with standard deviation $\sigma_{\triangle x'}$ and normalized tilt $\boldsymbol{\Delta \varphi'}_x = \boldsymbol{\Delta \varphi}_x/(a/f)$ with standard deviation $\sigma_{\triangle \varphi'_x}$ as stochastic parameters. Solid lines are for an optimum design parameter $\chi = \chi_0$, broken lines are for $\chi = 0.7\chi_0$.

Fig. 6. Coupling geometry with a pigtailed collimator. A quarter-pitch GRIN-lens is directly attached to the fiber end. It effectively increases the modefield radius from $w_{\mathcal{B}}$ to $w_{\mathcal{C}}$.

Fig. 7. Lines of constant mean coupling efficiency $\langle \boldsymbol{\eta} \rangle = 0.75\eta_0$ as a function of the standard deviations of the normalized lateral misalignment $\sigma_{\triangle x}/w_{\mathcal{B}}$ and the normalized tilt $\sigma_{\triangle \varphi_x}/(a/f) = \sigma_{\triangle \varphi_x} \cdot \pi w_{\mathcal{B}}/(\lambda \chi)$ for several magnification factors A.

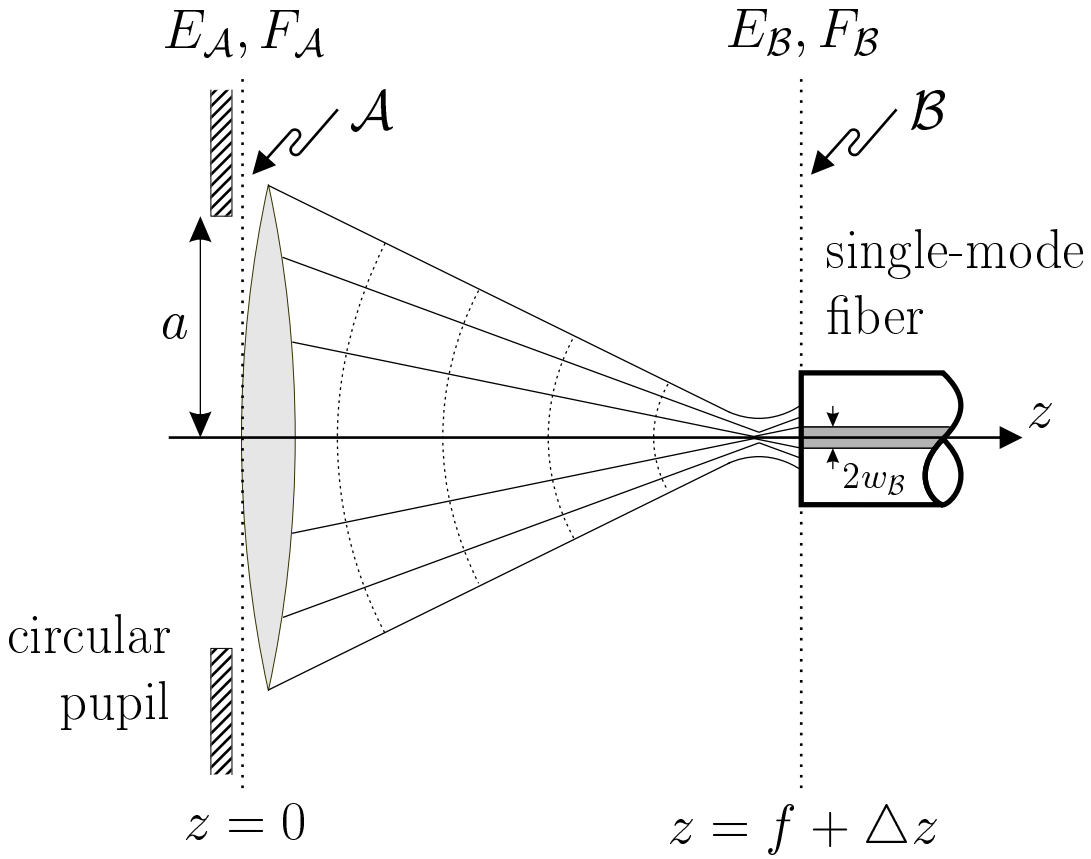

Figure 1, O. Wallner, Appl. Opt.

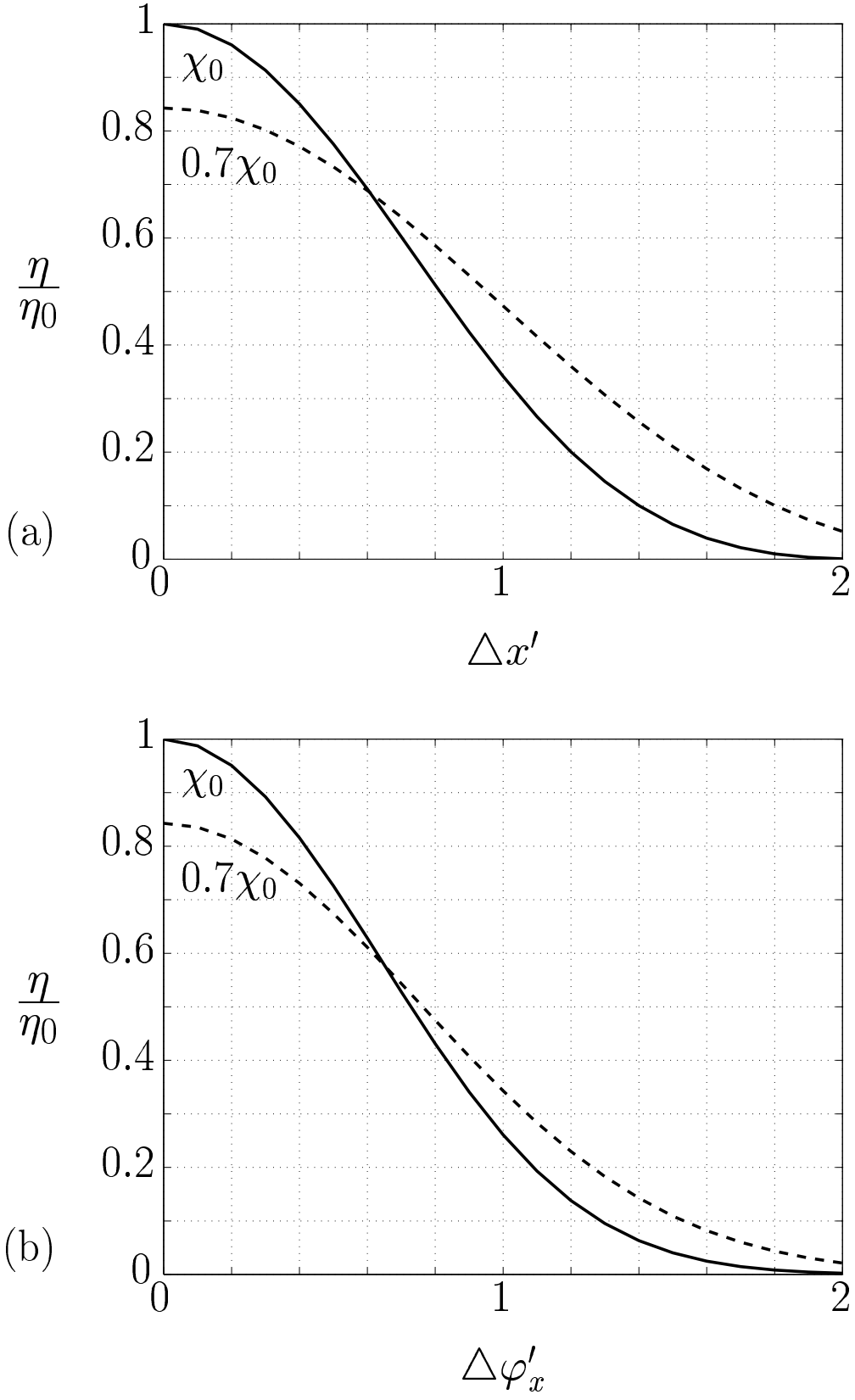

Figure 2, O. Wallner, Appl. Opt.

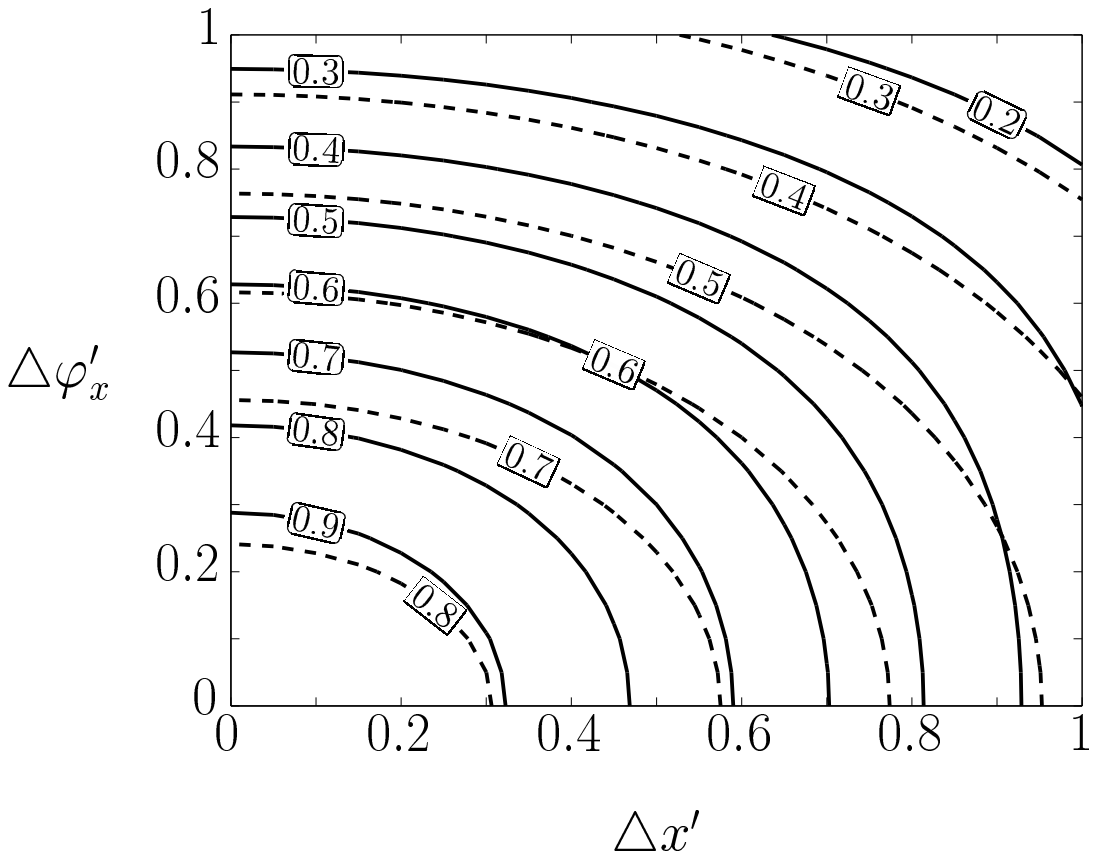

Figure 3, O. Wallner, Appl. Opt.

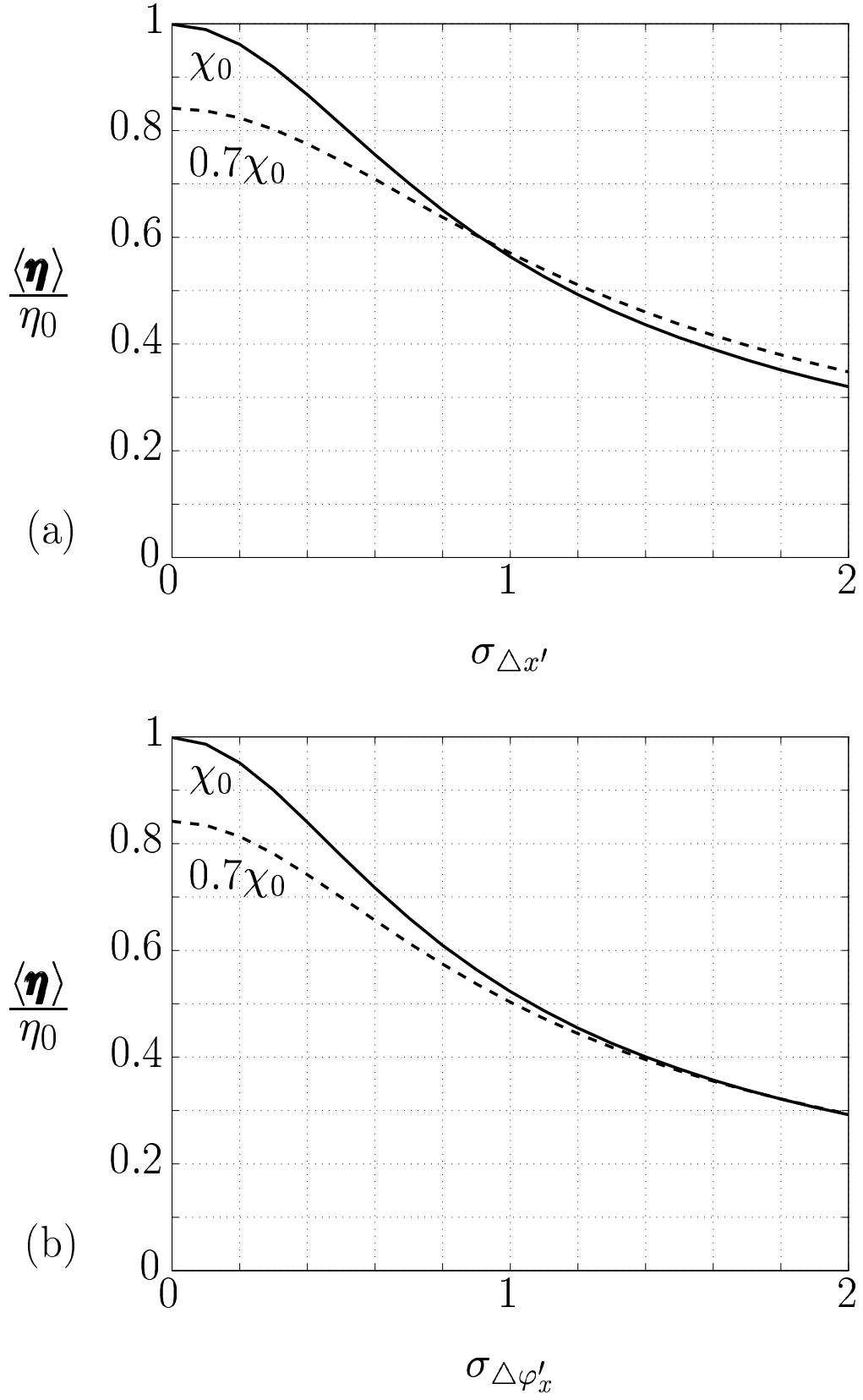

Figure 4, O. Wallner, Appl. Opt.

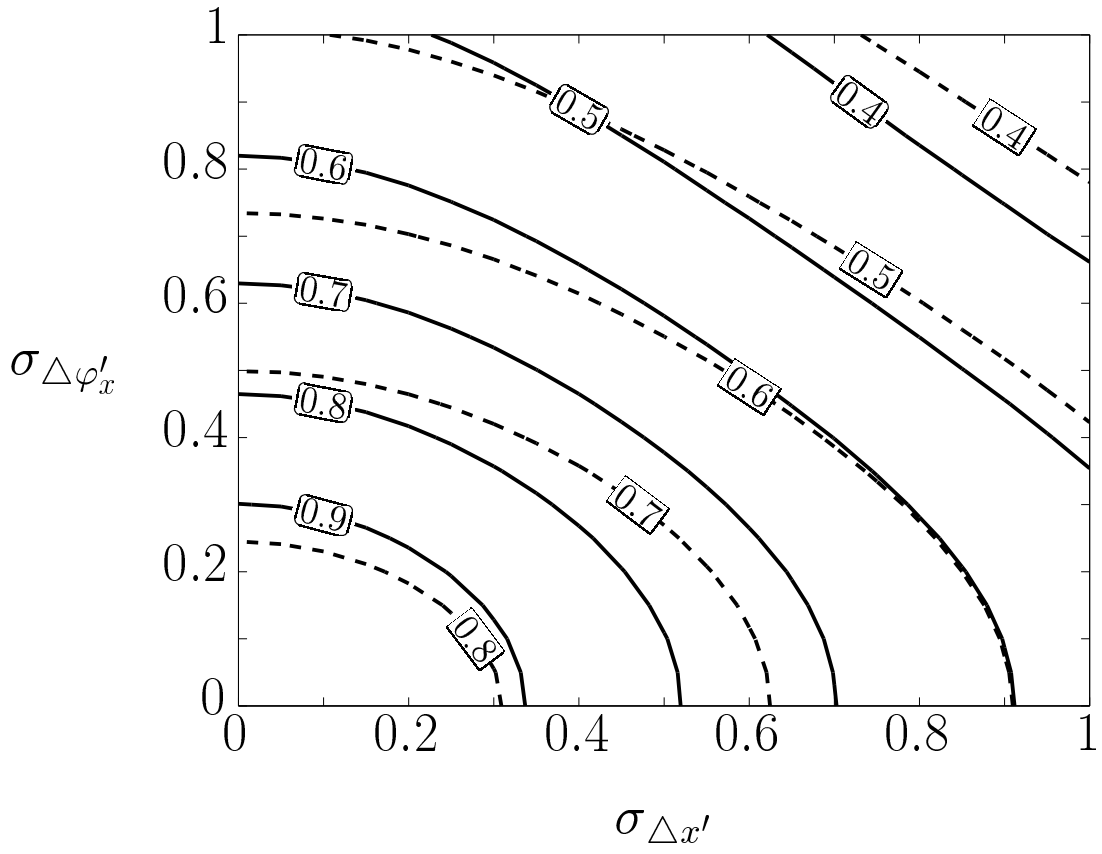

Figure 5, O. Wallner, Appl. Opt.

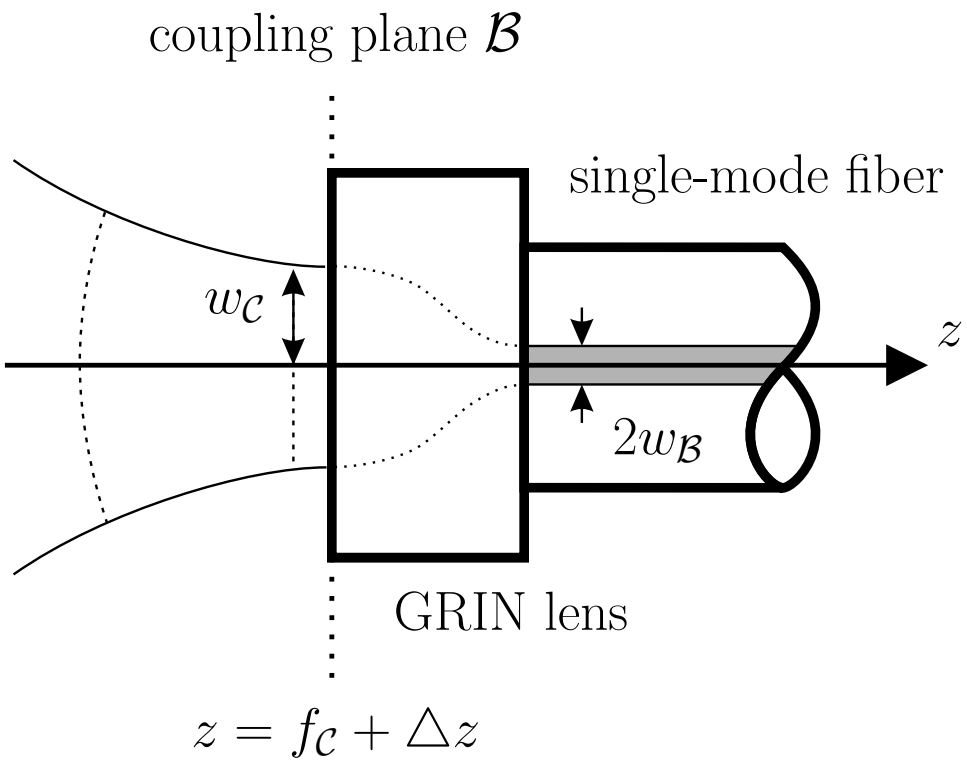

Figure 6, O. Wallner, Appl. Opt.

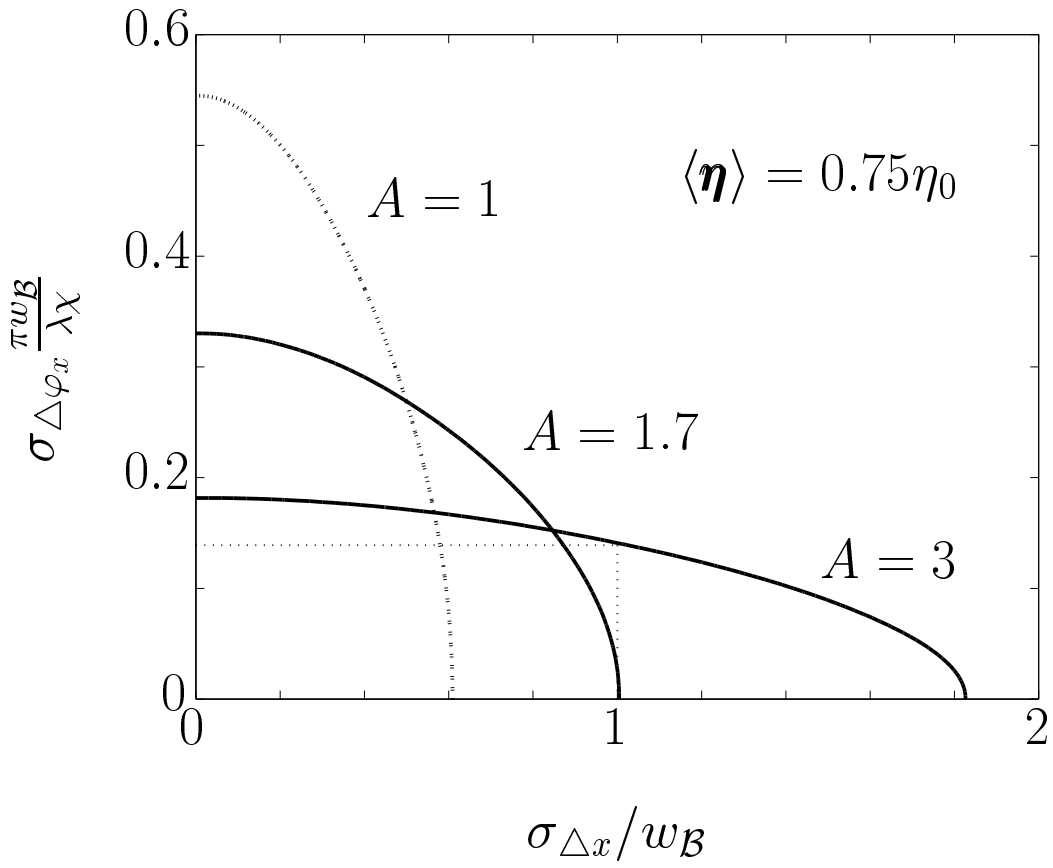

Figure 7, O. Wallner, Appl. Opt.